

Numerical solution analysis of water flow in porous medium under phase changes due to evaporation

Juliana Arbelaez Gaviria and Michal Kuraz

Department of Water Resources and Environmental Modelling
Czech University of Life Sciences Prague

Introduction

Evaporation (ET) is a dynamic and nonlinear process that incorporates various internal transport mechanisms, which is essential in the unsaturated zone in arid regions under low soil moisture conditions. FAO Penman-Monteith (PM) equation is the most widespread method to estimate the evaporation rate in saturated soils. This approach can be implemented as a boundary condition for the Richards' equation and related to the evaporation rate with the water content in the soil. However, the PM equation is not valid when the soil moisture is low, and the vapor flux is an essential component of the total water flux. In this case, the governing equations are formed out of the coupled Richards' equation with the heat transport, where the boundary conditions originate from the surface energy balance and the evaporation rate (Saito et al., 2006; Sakai et al., 2011).

Methodology

Two models were implemented in the Dual Richards' Unsaturated Equation Solver (DRUtES). The first model accounts for surface evaporation by coupling the Richards' equation and the Penman-Monteith equation

$$\nabla \cdot (\mathbf{K}(\theta) \nabla h) + \frac{\partial K_{zz}(\theta)}{\partial z} = C(h) \frac{\partial h}{\partial t} \quad (1)$$

The initial condition

$$h(\mathbf{x}, t_0) = h_0(\mathbf{x}) \quad \forall \mathbf{x} \in \Omega \quad (2)$$

The surface boundary condition

$$\mathbf{K}(h) \left(\frac{\partial h(\mathbf{x}, t)}{\partial \mathbf{n}} + n_3 \right) = q_{\Gamma_{surf}}(t) \quad \forall (\mathbf{x}, t) \in \Gamma_{surf} \times [0, T] \quad (3)$$

Including the actual evapotranspiration

$$q_{\Gamma_{surf}}(t) = \begin{cases} r(t) - ET_o(t) & \text{if } r(t) - ET_o(t) \geq 0 \\ r(t) - ET_o(t) \theta_l(h)^{2/3} & \text{if } r(t) - ET_o(t) < 0 \end{cases} \quad (4)$$

And the Penman-Monteith equation for the evaporation rate

$$ET_o = \frac{0.408 \Delta (R_n - G) + \gamma \frac{900}{T+273} u_2 (e_s - e_a)}{\Delta + \gamma (1 + 0.34 u_2)} \quad (5)$$

The second model accounts for sub-surface evaporation by coupling a modified Richards' equation and the heat equation

$$\begin{cases} C_h \frac{\partial h}{\partial t} = \nabla \cdot (\mathbf{K}_{Th} \nabla h) + \nabla \cdot (\mathbf{K}_{TT} \nabla T) \\ \quad + \nabla \cdot (\mathbf{K}_{Th} \nabla z) - \frac{\partial \theta_v}{\partial t} \quad \forall \mathbf{x} \in \Omega \\ C_T \frac{\partial T}{\partial t} = \nabla \cdot (\mathbf{B}_{TT} \nabla T) + \nabla \cdot (\mathbf{B}_{Th} \nabla h) \\ \quad - \nabla \cdot [(C_l \vec{q}_l + C_v \vec{q}_v) T] - L \frac{\partial \theta_v}{\partial t} \quad \forall \mathbf{x} \in \Omega \end{cases} \quad (6)$$

Initial condition for both partial differential equations

$$h(\mathbf{x}, t_0) = h_0(\mathbf{x}) \quad \forall \mathbf{x} \in \Omega \quad (7)$$

$$T(\mathbf{x}, t_0) = T_0(\mathbf{x}) \quad \forall \mathbf{x} \in \Omega \quad (8)$$

The surface boundary condition for the water equation

$$\| \vec{q}_v(\mathbf{x}, t) \|_{\mathbf{x}=\mathbf{n}} + \| \vec{q}_l(\mathbf{x}, t) \|_{\mathbf{x}=\mathbf{n}} = E_v(t) \quad \forall \mathbf{x} \in \Gamma_{surf} \times [0, T] \quad (9)$$

Including the evaporation rate

$$E_v(t) = \frac{Hr(h, T_s) \rho_{sv}(T_s) - RH_{air} \rho_{sv}(T_a)}{\rho_l r_a} \quad (10)$$

The surface boundary condition for the heat equation

$$-\kappa \frac{\partial T}{\partial \mathbf{n}} + C_v \| \vec{q}_v \|_{\mathbf{x}=\mathbf{n}} = -G - L \| \vec{q}_v \|_{\mathbf{x}=\mathbf{n}} \quad \forall \mathbf{x} \in \Gamma_{surf} \times [0, T] \quad (11)$$

Including the surface energy balance

$$R_n - H_s - LE_v + G = 0 \quad (12)$$

h : pressure head [m]. $\mathbf{K}(\theta)$: unsaturated hydraulic conductivity [ms^{-1}]. $C(h)$: retention water capacity [m^{-1}]. t : time [s]. $q_{\Gamma_{surf}}(t)$: boundary surface flux [ms^{-1}]. $r(t)$: rain intensity [ms^{-1}]. θ_l : liquid water content [-]. ET_o : the reference evapotranspiration [mm day^{-1}]. R_n : the net radiation [$\text{MJ m}^{-2} \text{day}^{-1}$]. G : soil heat flux density [$\text{MJ m}^{-2} \text{day}^{-1}$]. u_2 : the wind speed measured at 2 m height [ms^{-1}]. e_s : saturation vapor pressure [kPa], e_a : the actual vapor pressure [kPa]. Δ : the slope vapor pressure curve [$\text{kPa}^\circ\text{C}^{-1}$]. γ : psychrometric constant [$\text{kPa}^\circ\text{C}^{-1}$]. T : temperature $^\circ\text{C}$. H_s : sensible heat [$\text{MJ m}^{-2} \text{day}^{-1}$]. L is the latent heat, \vec{q}_v : vapor flux [ms^{-1}]. \vec{q}_l : liquid flux [ms^{-1}]. θ_v : vapor water content [-]. $Hr(h, T_s)$: soil relative humidity [-]. ρ_{sv} : saturation vapor density [kg m^{-3}]. T_s : soil temperature $^\circ\text{C}$. T_a : air temperature $^\circ\text{C}$. RH_{air} : air relative humidity [-]. ρ_l : liquid water density [kg m^{-3}]. r_a : aerodynamic resistance to water vapor flow [sm^{-1}]. \mathbf{n} : normal vector to the surface.

Results

A 20 cm long soil profile was used to perform the numerical experiments in 1D. The simulated experiments had total simulation time of 14 days, where the hydraulic properties and the numeric parameters were consistent across all the simulations. Two scenarios were proposed under controlled meteorological conditions.

- The first scenario is known as a dark condition where no incoming shortwave radiation was considered, $R_s = 0$.
- The second scenario is characterized by a constant incoming shortwave radiation, $R_s = \text{constant}$.

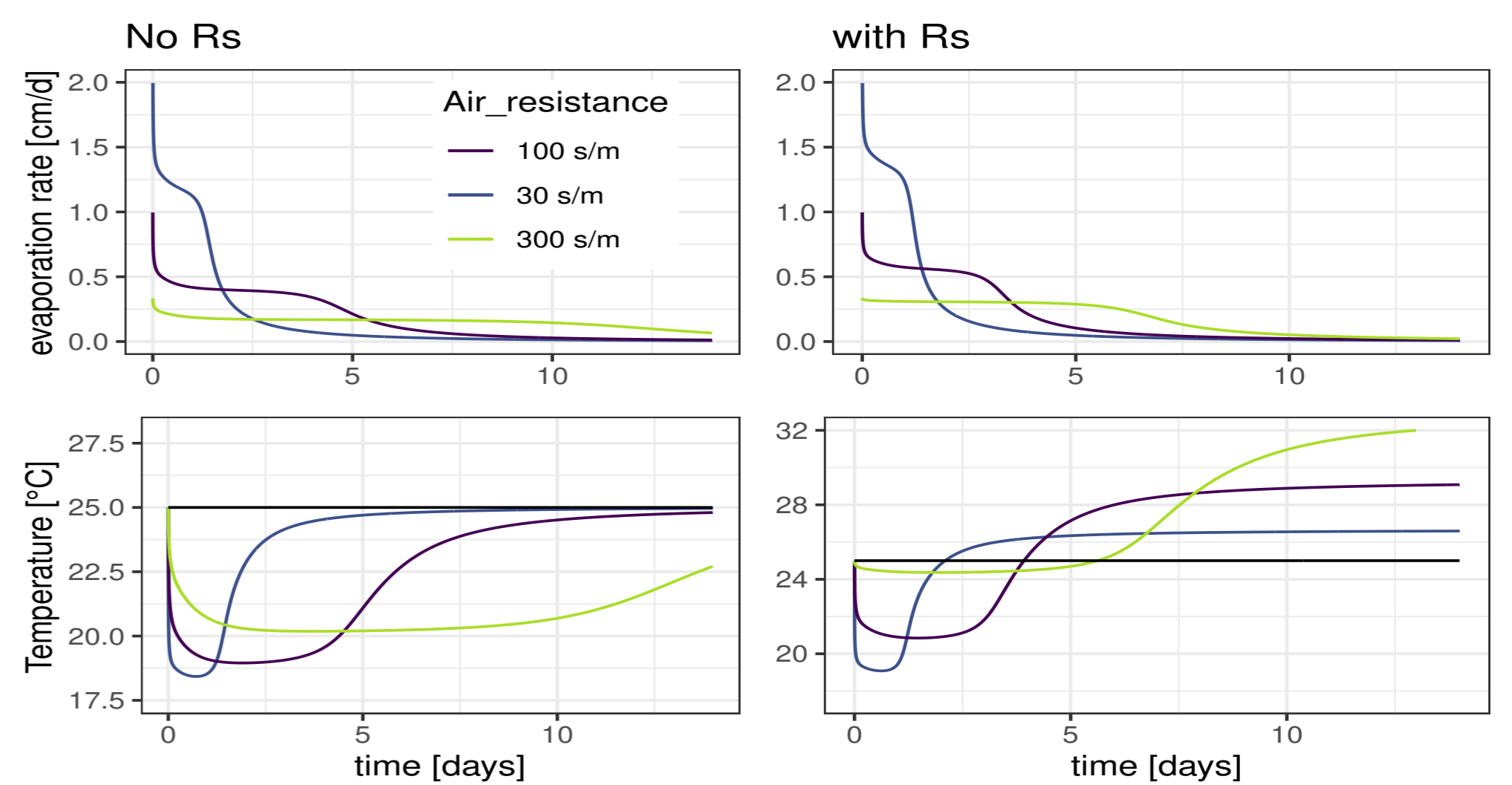
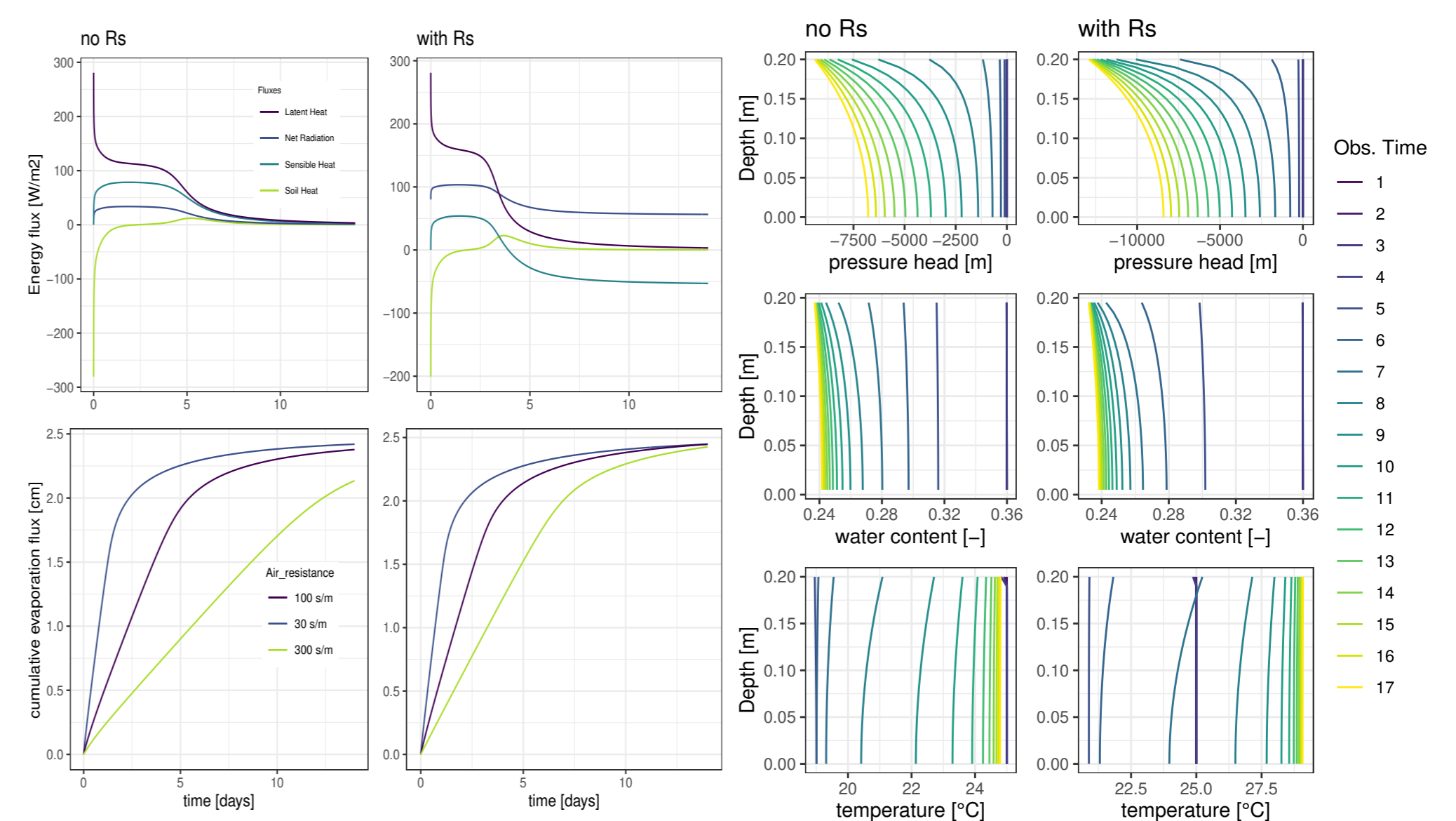


Figure 1: Results of numerical simulation of the evaporation rates (upper) and soil surface temperature (bottom) time series for different values of the air resistance r_a , without shortwave radiation (left) and with shortwave radiation (right).



(a) Components of the surface energy balance (upper) and cumulative evaporation flux (bottom) without shortwave radiation (left) and with shortwave radiation (right) with different values of air resistance r_a . (b) Distribution of pressure head (top), volumetric water content (middle), and temperature (bottom) at different simulation times without shortwave radiation (left) and with shortwave radiation (right).

Figure 2: Results of the numerical simulations with an aerodynamic resistance $r_a = 100 \text{ s/m}$.

Conclusions

- The numerical implementation of the Penman-Monteith method as the boundary condition of the classical Richards equation was presented.
- The application of the coupled model of heat and water flow was implemented in the free software Dual Richards Unsaturated Equation Solver (DRUtES).
- Two scenarios were designed to test the performance of both models under a controlled meteorological environment and the impact of the evaporation rate on the pressure head and water content.

References

- Saito, H., Simunek, J., & Mohanty, B. P. (2006). Numerical analysis of coupled water, vapor, and heat transport in the vadose zone. *Vadose Zone Journal*, 5(2), 784–800.
- Sakai, M., Jones, S. B., & Tuller, M. (2011). Numerical evaluation of subsurface soil water evaporation derived from sensible heat balance. *Water Resources Research*, 47(2).